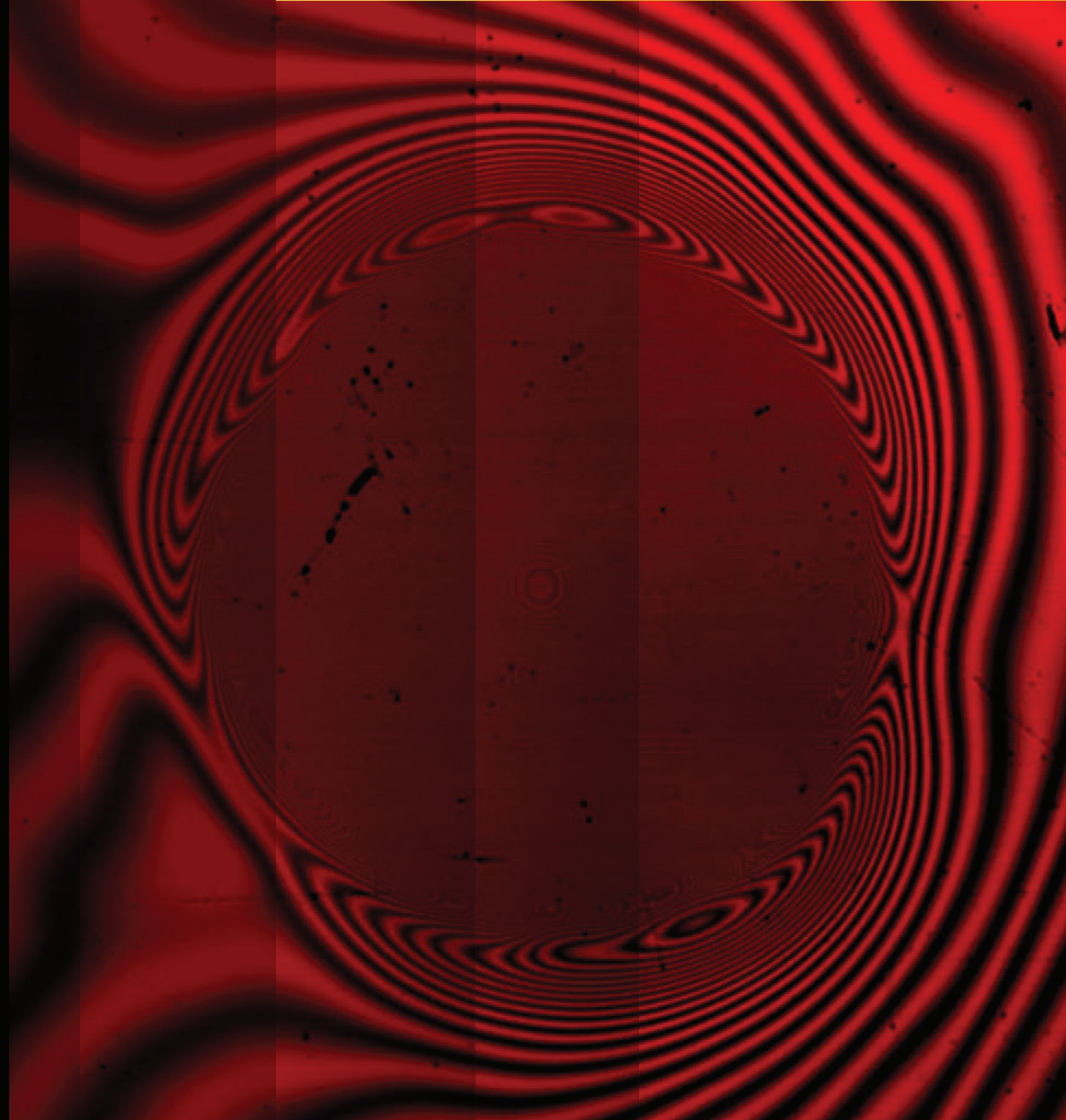


MAGIC AT INTERFACES

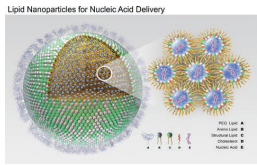
Sushanta K. Mitra

*Micro & Nano-scale Transport Laboratory,
Waterloo Institute for Nanotechnology,
Department of Mechanical & Mechatronics Engineering,
University of Waterloo, Waterloo, N2L 3G1, Ontario, Canada*



APPLICATIONS OF ENCAPSULATION

Pharmaceuticals



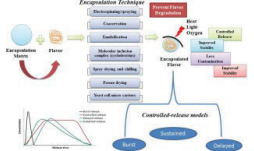
Samaridou, E., et al. *Adv. Drug Deliv. Rev.* **2020**, 154, 37-63.

Nutraceuticals



Source: pexels.com

Food and flavors



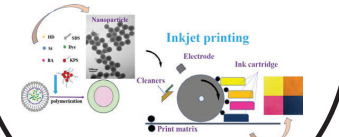
Premjit, Y., et al. *Food Res. Int.* **2022**, 110879.

Cosmetics and personal care



Source: Google

Inkjet printing

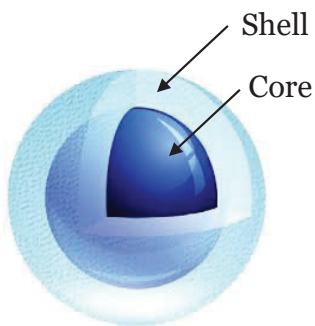


Li, J., et al., *ACS Omega* **2018**, 3, 7, 7380-7387

But why a new encapsulation technique?



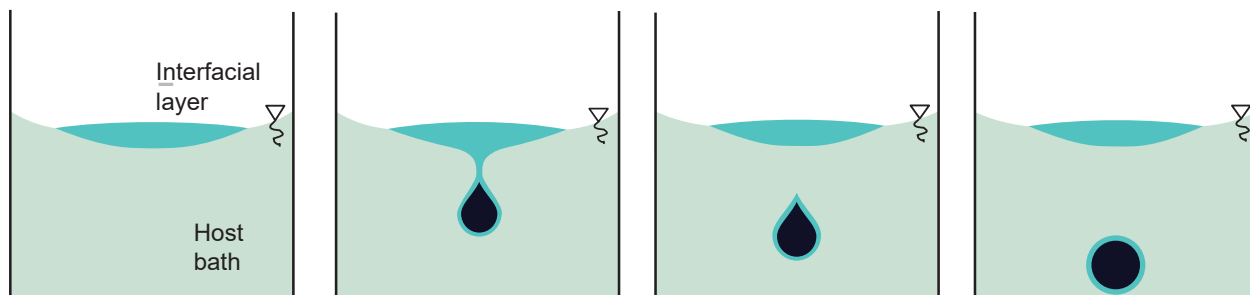
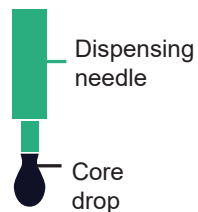
S. Misra



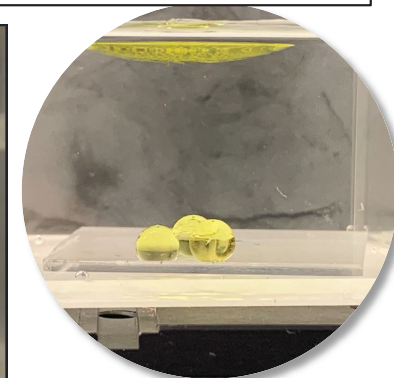
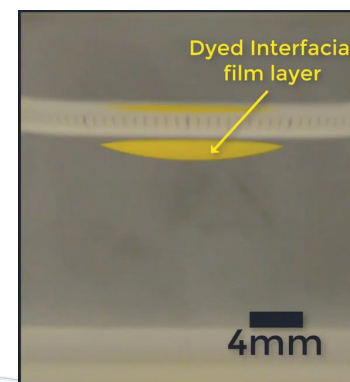
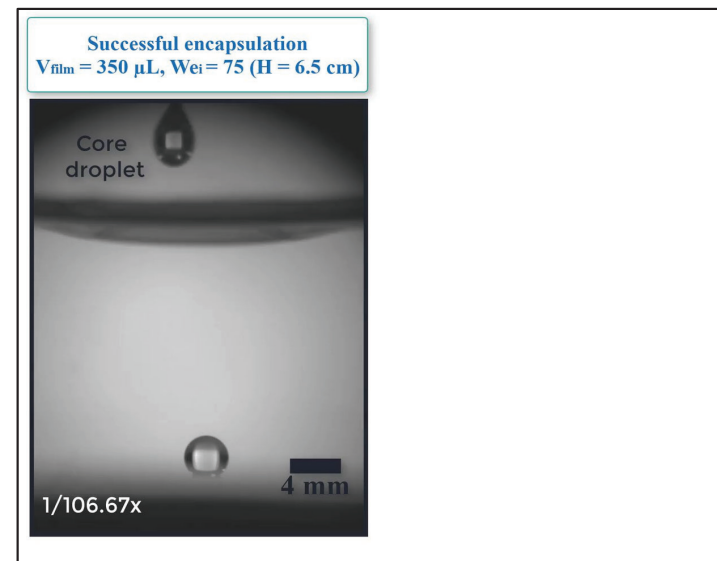
Existing encapsulation methods are either –

- Very case specific, with limited flexibility regarding material selection
- Restrictive in the range of applicability
- Involves intricate material processing or handling steps
- Requires complex and expensive infrastructure
- Simple methods offer limited control on dosage size

Encapsulation with an interfacial liquid layer: a novel liquid-based wrapping



- Ultrafast (~ 50 ms/encapsulation) and therefore scalable
- Surface tension driven wrapping – minimally restrictive on materials
- Controllably produces stable monodispersed encapsulated drops
- Allows multilayer encapsulation
- Allows precise shell thickness control (~ 500 nm – 2 mm) by shell volume control
- Simple, executable as a table-top experiment



S. Mitra et al., *Journal of Colloid and Interface Science*, 2020, 558, 334-344.

S. Mitra et al., *U.S. Patent Application No. 17/432,848*, 2022.

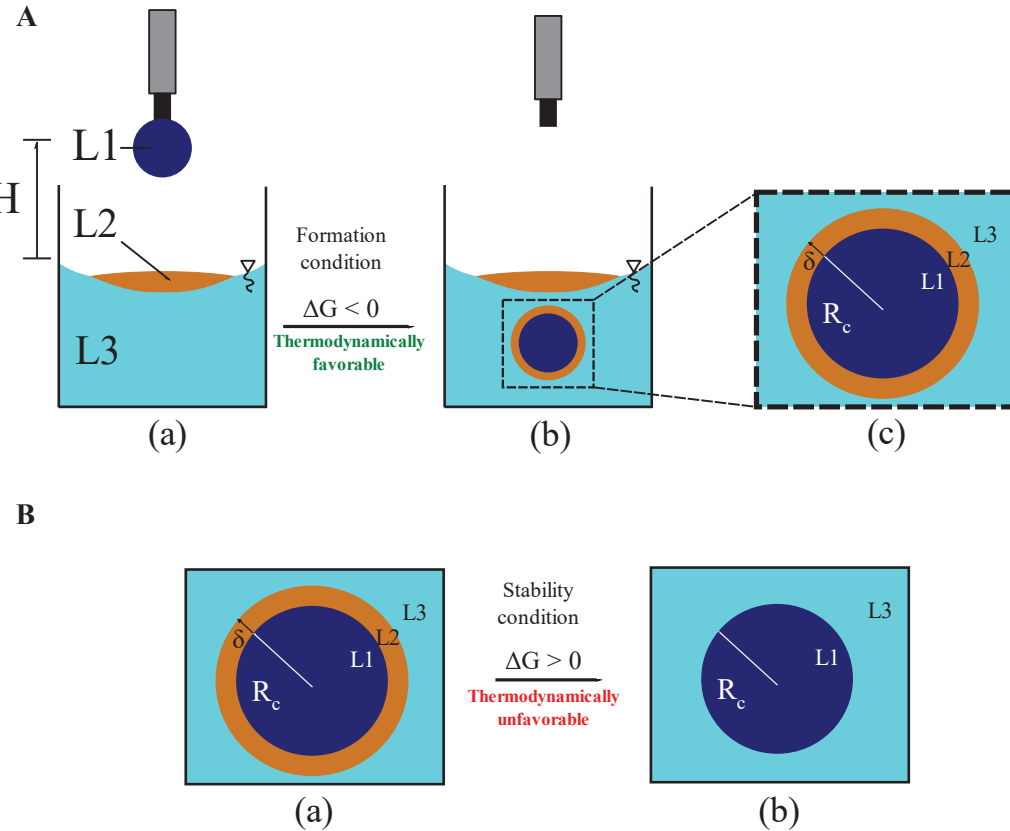
MAGIC AT INTERFACES

PAGE 3



UNIVERSITY OF
WATERLOO

A thermodynamic understanding of the encapsulation process



Thermophysical requirements:

- $\rho_1 > \rho_3 > \rho_2$
- L2 and L3 are physico-chemically compatible (i.e., unreactive, immiscible).

❖ Condition for formation of encapsulated drop:

$$\Delta G_{\text{formation}} = G_{A(b)} - G_{A(a)} \approx 4\pi R_c^2(\gamma_{12} + \gamma_{23} - \gamma_1) - \frac{4}{3}\pi R_c^3 \rho_1 g H < 0$$

$$\rightarrow (\gamma_{12} + \gamma_{23} - \gamma_1) < 0 \quad [:: H \text{ is a positive variable}]$$

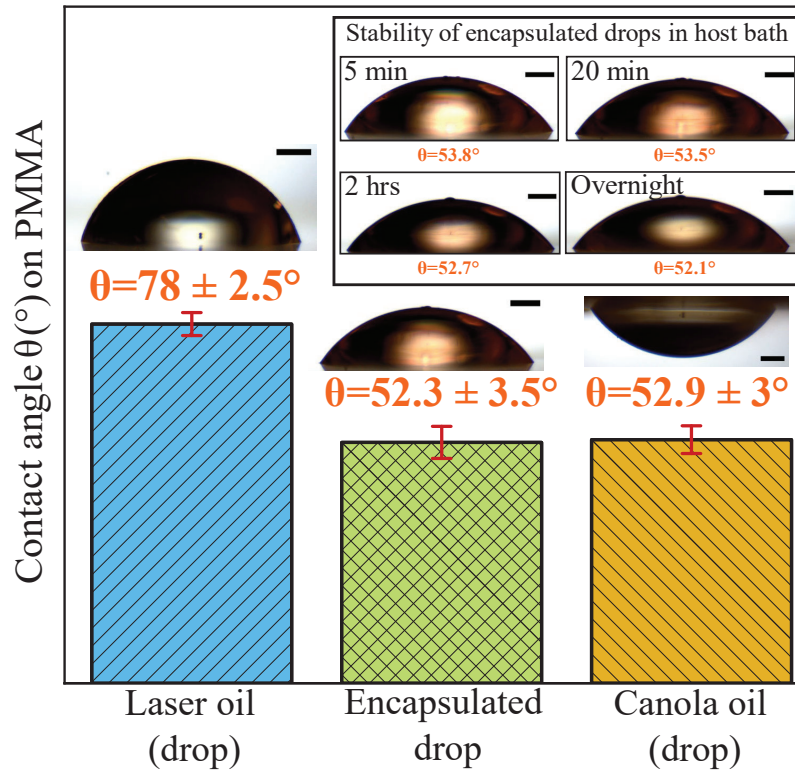
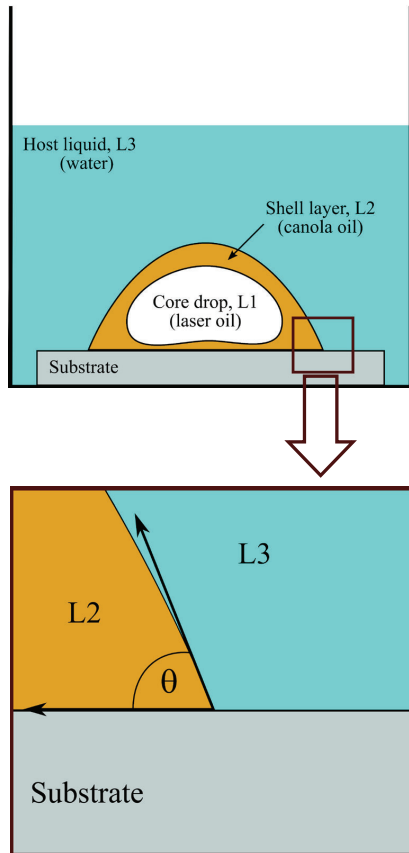
❖ Condition for stability of encapsulated drop:

$$\Delta G_{\text{detachment}} = G_{B(b)} - G_{B(a)} \approx 4\pi R_c^2(\gamma_{13} - \gamma_{12} - \gamma_{23}) > 0$$

$$\rightarrow (\gamma_{13} - \gamma_{12} - \gamma_{23}) > 0$$

S. Misra et al., *Journal of Colloid and Interface Science*, 2020, 558, 334-344.
 S. Mitra et al., U.S. Patent Application No. 17/432,848, 2022.

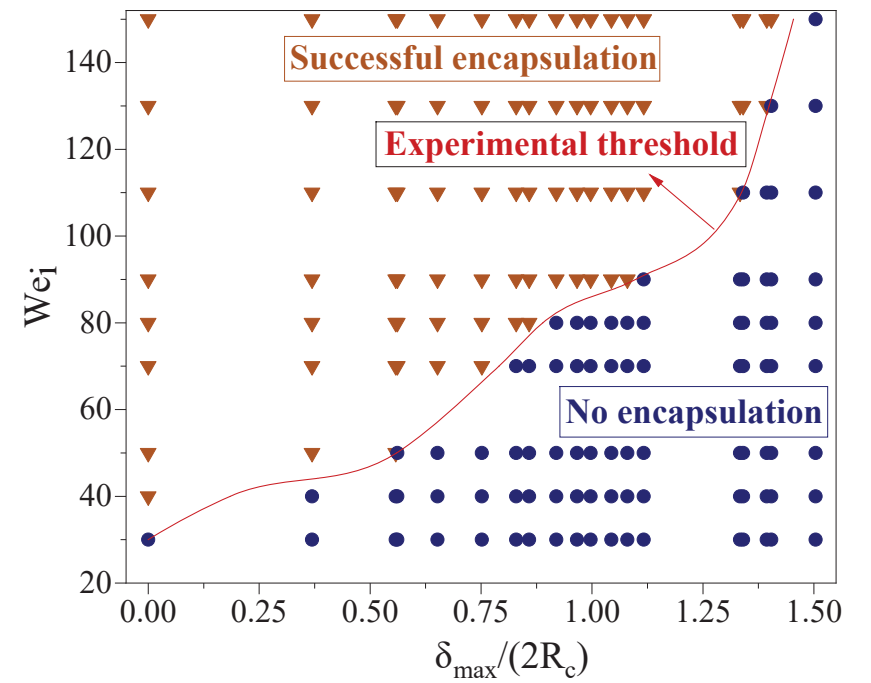
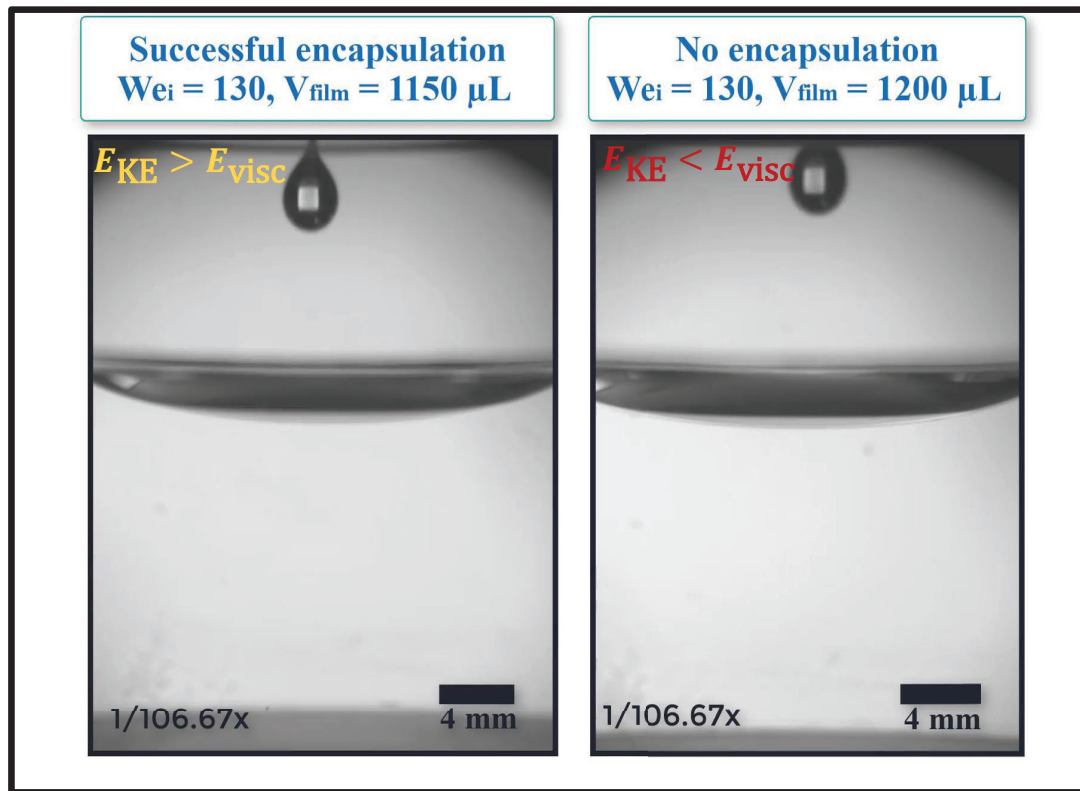
Wetting Signature



Resemblance in underwater wetting signature between encapsulated drop and shell liquid confirms integrity of wrapping

Role of viscous dissipation: deviation from ideal thermodynamic estimate

- $(\gamma_1 > \gamma_{12} + \gamma_{23})$ is not sufficient for encapsulation as viscous dissipation remains unaccounted in equilibrium thermodynamic analysis.
- Encapsulation is possible only if $E_{KE} > E_{visc}$.



▼ Successful encapsulation
 ● No encapsulation

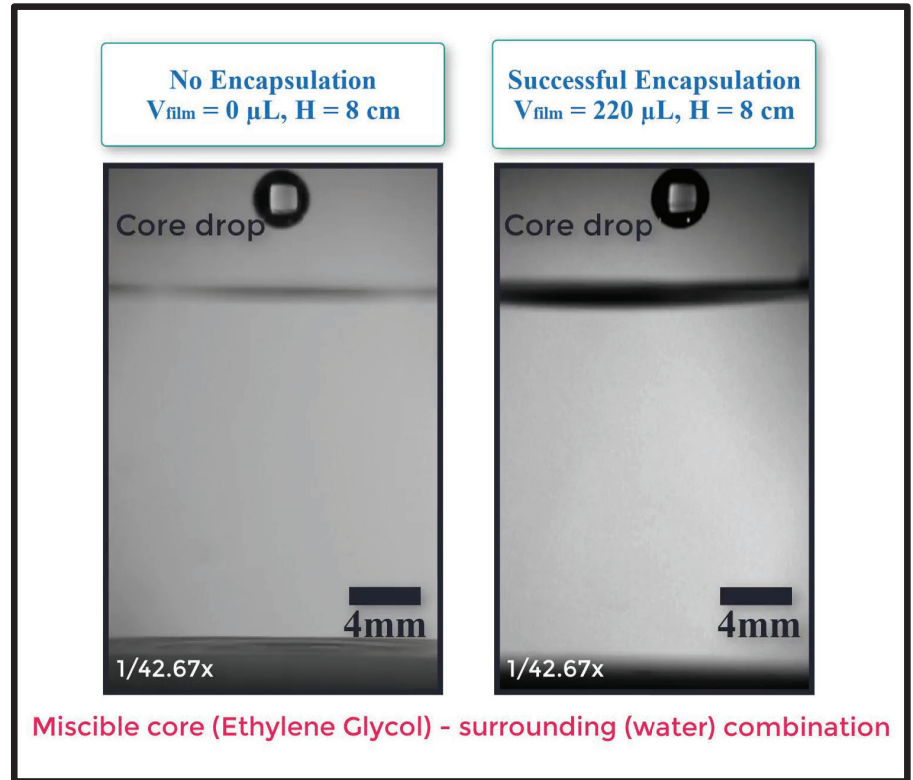
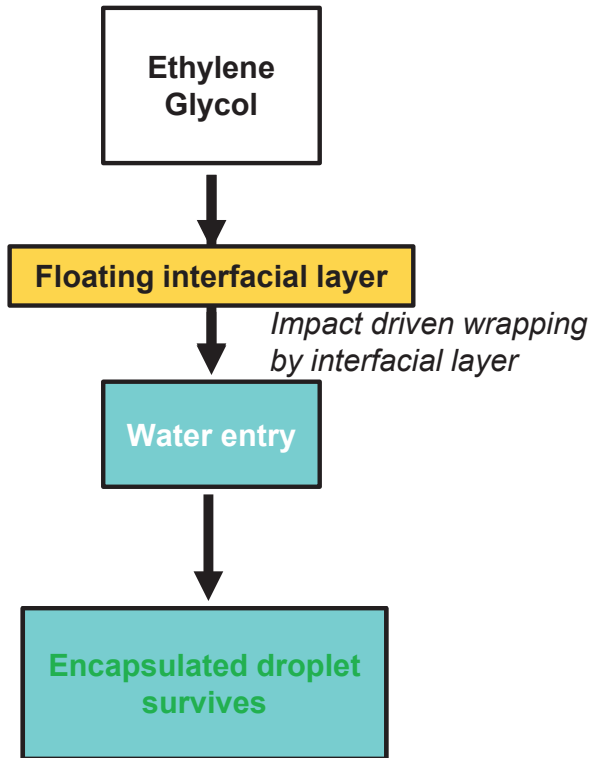


UNIVERSITY OF WATERLOO

S. Misra et al., *Journal of Colloid and Interface Science*, 2020, 558, 334-344.

S. Mitra et al., *U.S. Patent Application No. 17/432,848*, 2022.

Applicability in providing protection from aggressive surrounding



The wrapping layer provides effective protection to Ethylene glycol drop (water soluble) from surrounding water medium

S. Misra et al., *Journal of Colloid and Interface Science*, 2020, 558, 334-344.
S. Mitra et al., *U.S. Patent Application No. 17/432,848*, 2022.

Demonstration of practical use cases - versatility

Encapsulated cargo inside liquid phase (e.g., flavoured beverages)

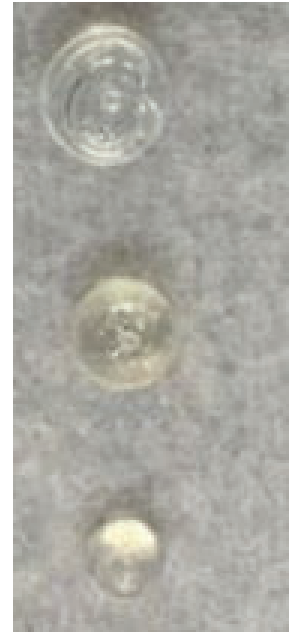
Honey in water

Honey in water

Maple syrup in water

Multiple encapsulated cargo

Individual extracted cargo



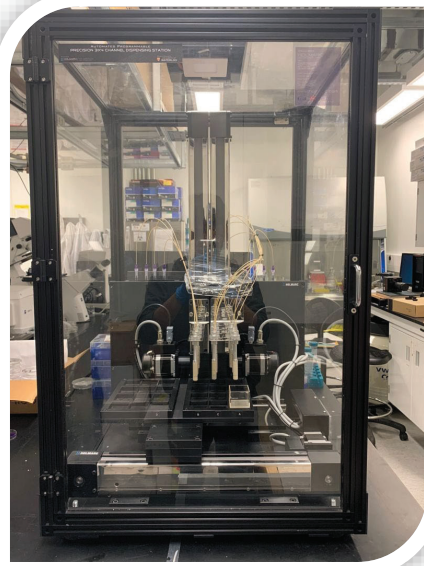
Shell-hardened (UV) capsules of varying sizes

- Efficient Control on shape and size of encapsulated cargo
- Perfectly spherical capsules!
- Excellent protection despite miscibility!

Commercialization pathway



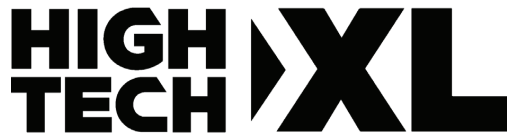
Fully functional High throughput commercial prototype



SLE Enterprises B.V.
High Tech Campus 27,
5656 AE Eindhoven, Netherlands

www.sle-enterprises.com

sushanta.mitra@sle-enterprises.com



SLE – Revolutionizing encapsulation machines



Nutraceutical

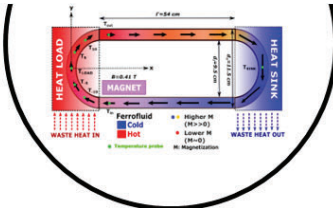

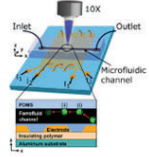
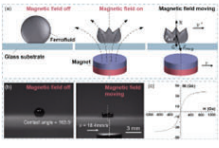
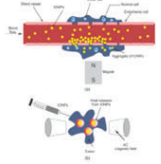


Food & beverages



APPLICATIONS OF FERROFLUID

- Ferrofluid is the colloidal solution made of magnetic nanoparticles (MNPs of size ~ 10 nm) coated with surfactants suspended in organic fluid/water/oil which offers contact-less magnetic manipulation.

Heat transfer	Sensors	Cell sorting	Microrobots	Drug delivery
				
Pattanaik, MS, et al., <i>Sci Rep</i> 2021, 11 (24167)	Chitnis, G., et al., <i>JMM</i> 2013, 23 (125031)	Kose A R., et al., <i>PNAS</i> 2009, 106 (21478-21483)	Chen D., et al., <i>APL</i> 2021, 118 (134101)	Asfer M., et al., <i>JMMM</i> 2017, 436 (47-56)



U. Banerjee



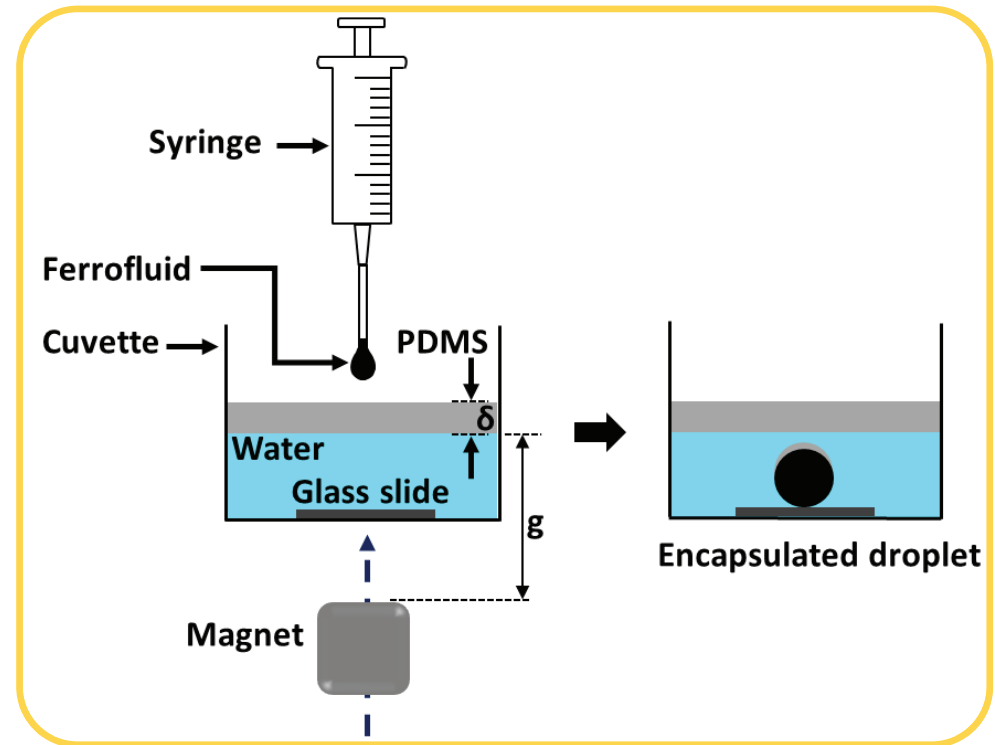
S. Misra

Research Problem

Magnet-assisted encapsulation of ferrofluid inside a PDMS shell

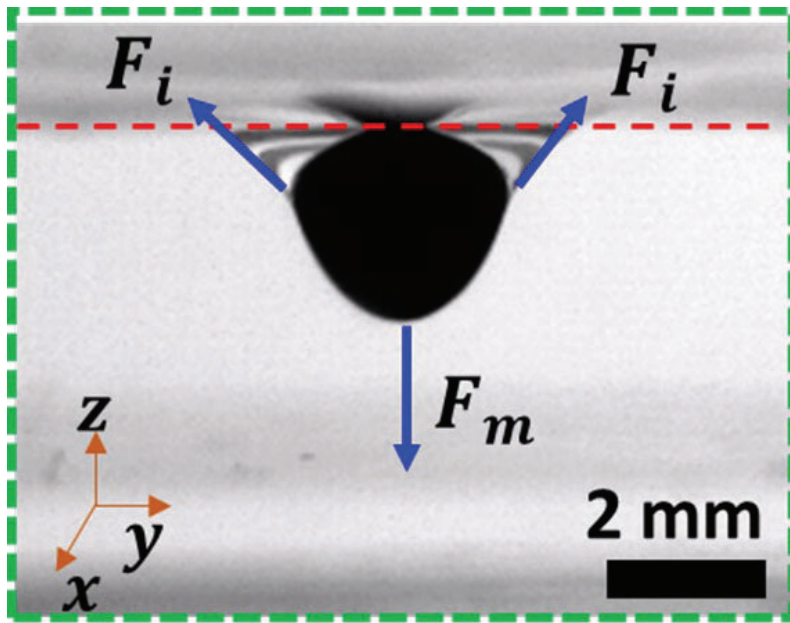
Research Questions

- How magnetic field can be tuned for successful encapsulation
- What is the criteria of successful encapsulation

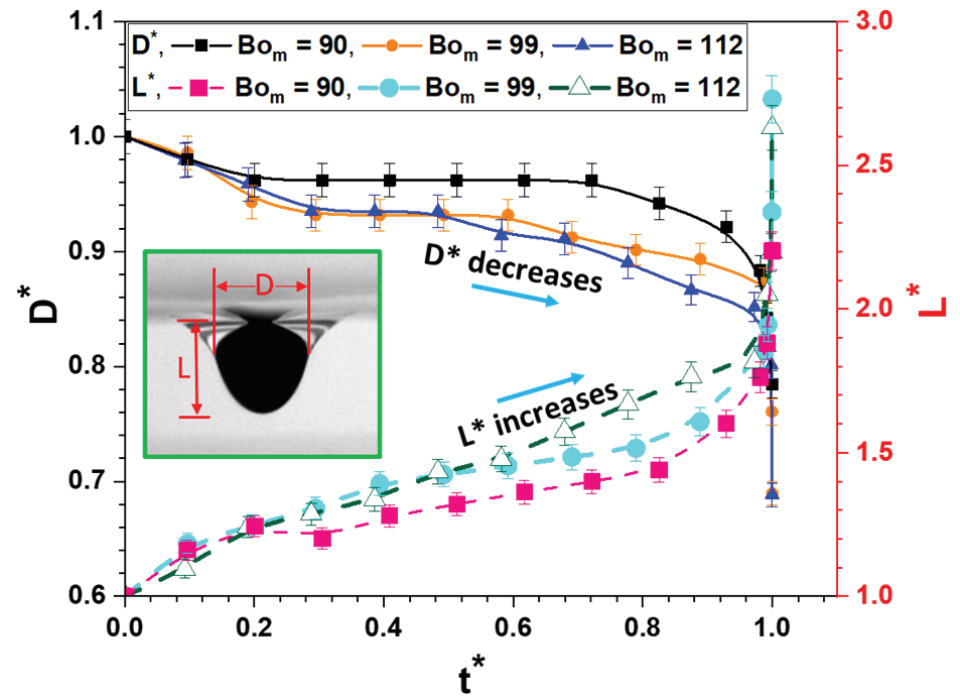


U. Banerjee*, S. Misra* & S.K. Mitra, *Adv. Mater. Interfaces* **2022**, 9, 21, 2200288

Shape evolution of the Ferrofluid-PDMS interface



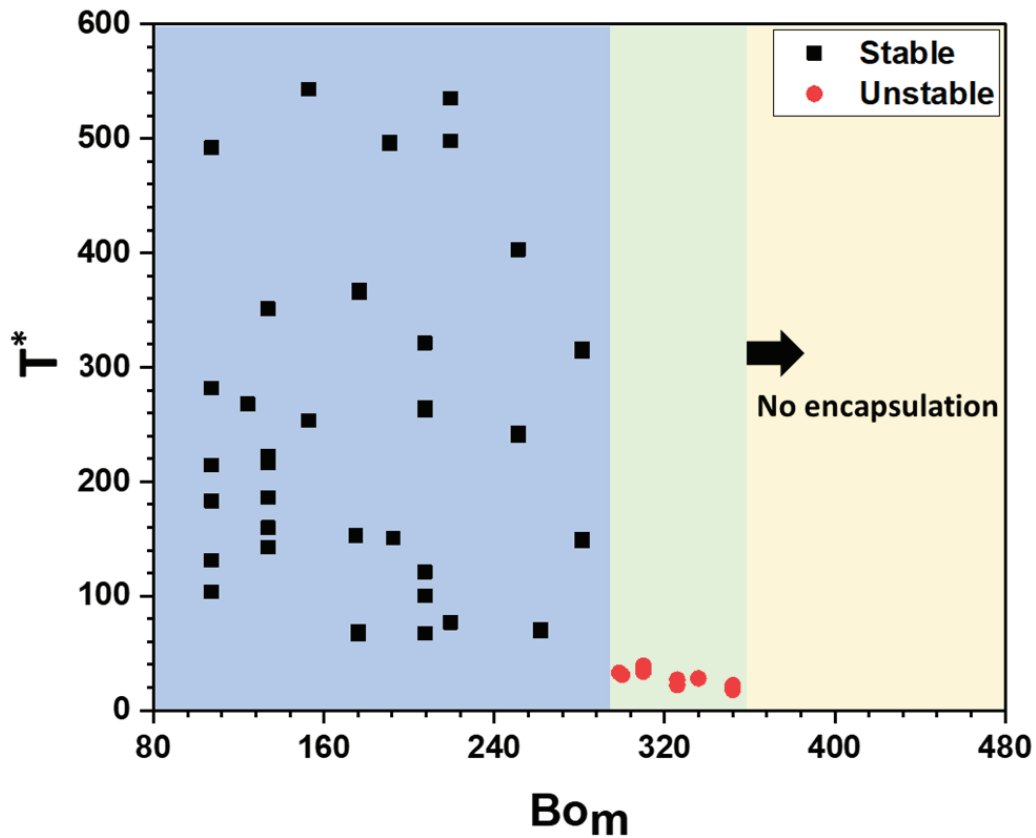
Interplay of forces



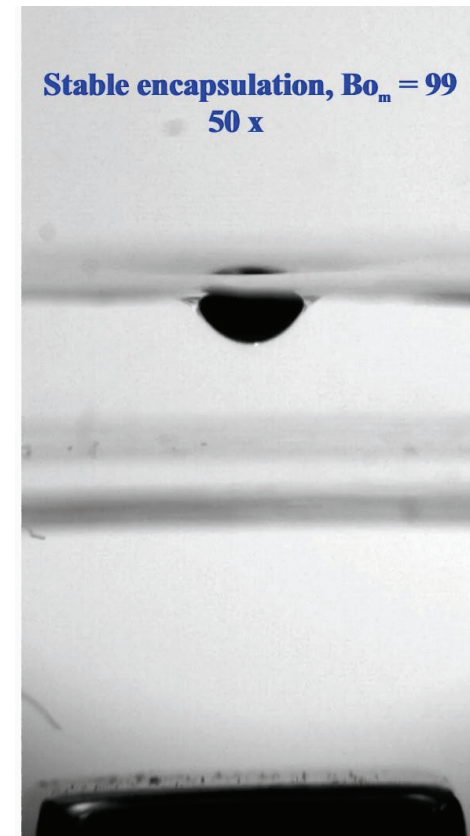
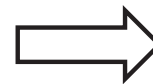
$$\triangleright L^* = \frac{L}{L_0}, D^* = \frac{D}{D_0}, t^* = \frac{t}{T}, Bo_m = \frac{F_m}{F_i}$$

U. Banerjee*, S. Misra* & S.K. Mitra, *Adv. Mater. Interfaces* 2022, 9, 21, 2200288

Regimes of encapsulation

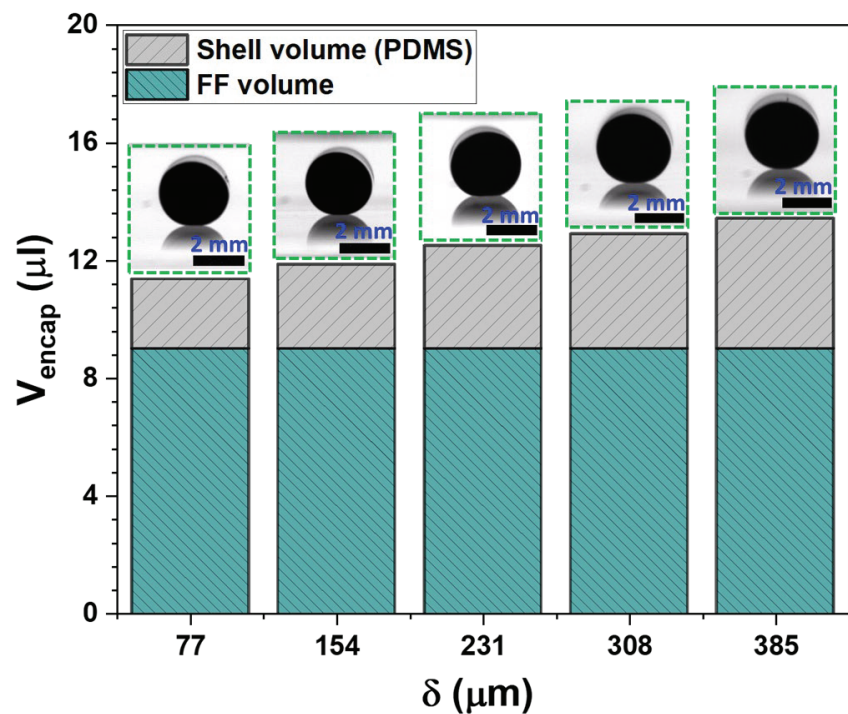


Regimes



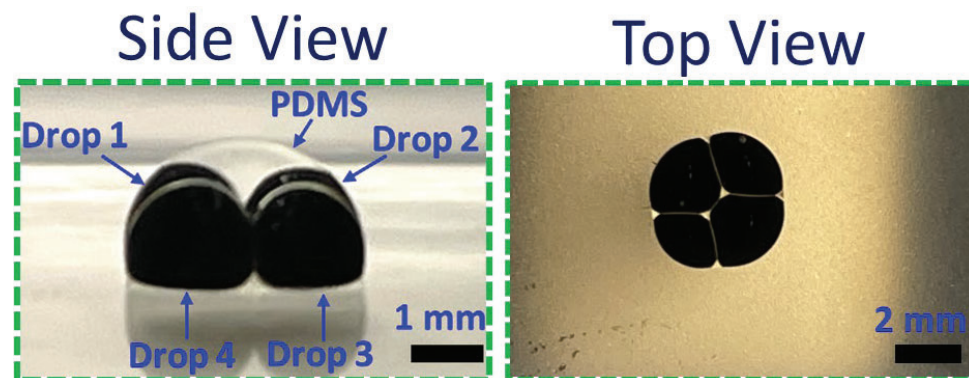
U. Banerjee*, S. Misra* & S.K. Mitra, *Adv. Mater. Interfaces* 2022, 9, 21, 2200288

Shell layer control and multiple encapsulation



Variation of shell thickness

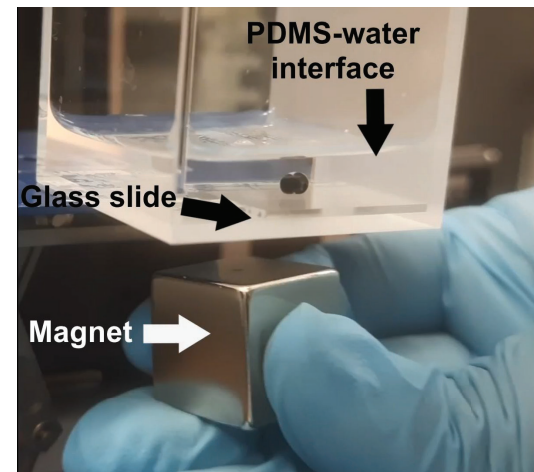
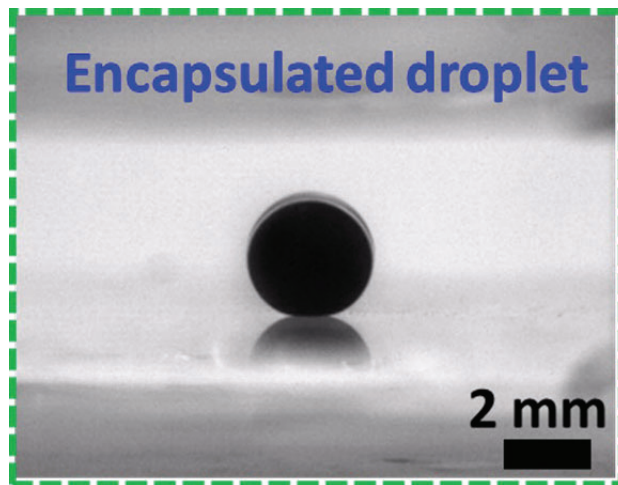
U. Banerjee*, S. Misra* & S.K. Mitra, *Adv. Mater. Interfaces* 2022, 9, 21, 2200288



Encapsulated cargo containing four ferrofluid droplets inside the PDMS shell

SUMMARY

- Magnet-assisted technique for encapsulating single and multiple ferrofluid droplets inside a PDMS shell
- Stable shell layer which is ensured from the under-water magnetic manipulation of the encapsulated cargo



U. Banerjee*, S. Misra* & S.K. Mitra, *Adv. Mater. Interfaces* **2022**, 9, 21, 2200288

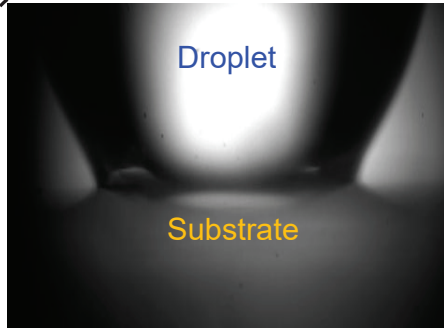
MAGIC AT INTERFACES

PAGE 15



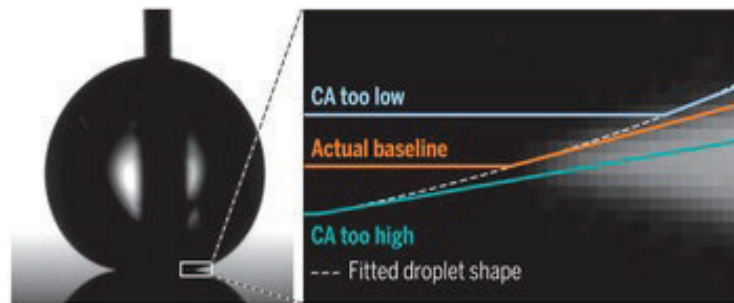
Why is direct adhesion measurement important?

Fundamental understanding



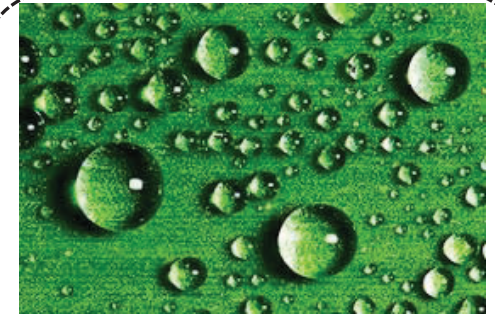
Source: MNT Lab

Uncertainties in Contact Angle Goniometry



Liu et. al, *Science*, 2019, **363**, 1147-1148,

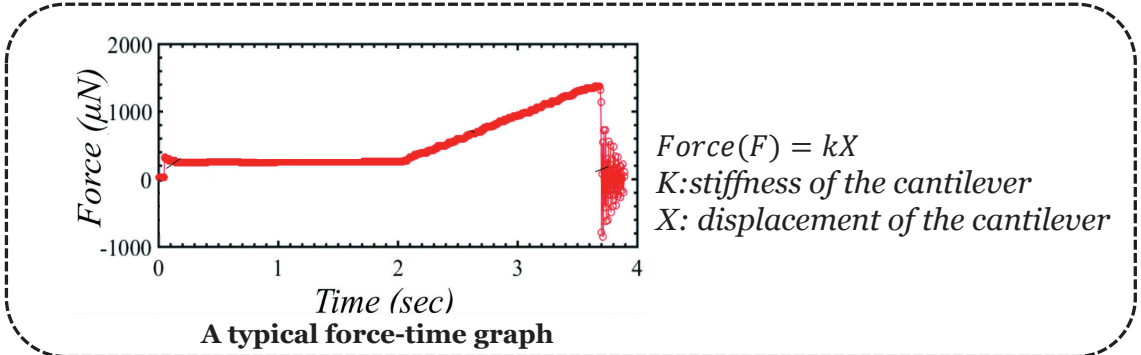
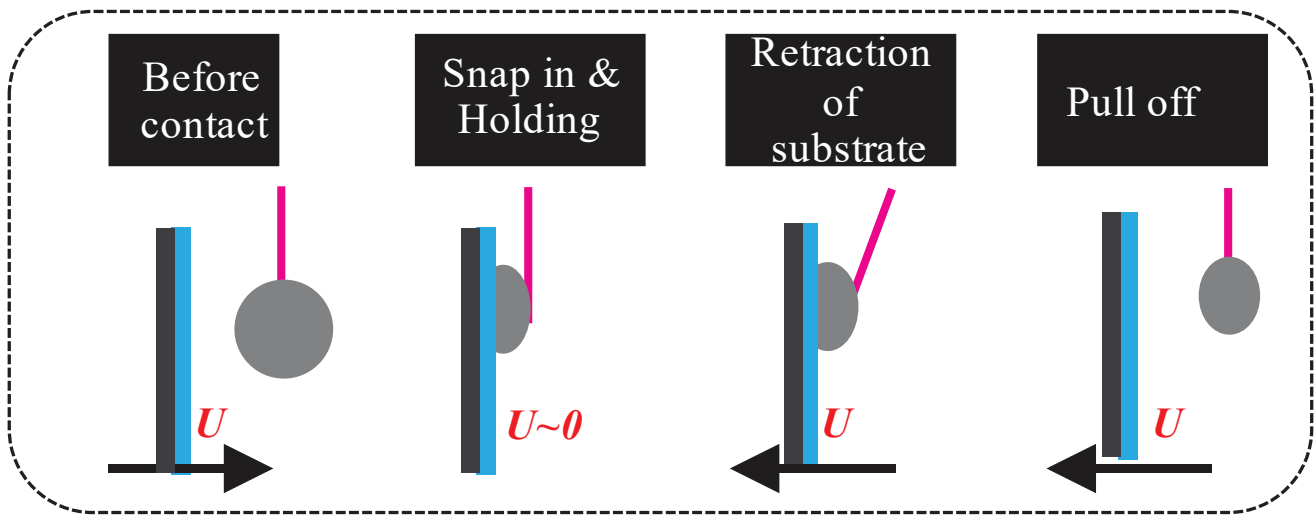
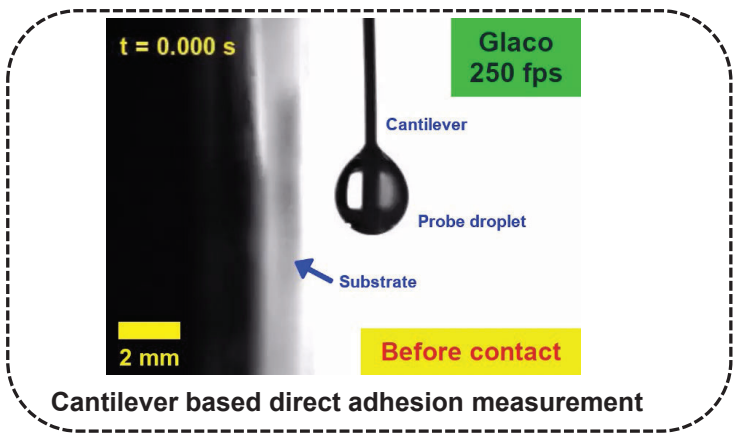
Development of coatings



Source:
<https://blog.paryleneconformalcoating.com/is-parylene-hydrophobic/>

S. Shyam*, S.Misra*, S.K. Mitra, *Journal of Colloid And Interface Science* **2022**, 630, 322-333

Cantilever based direct adhesion measurement

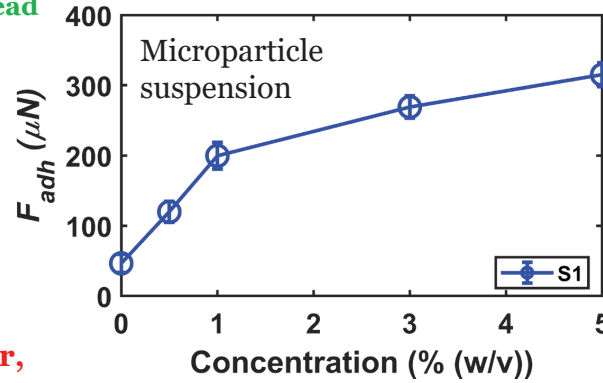
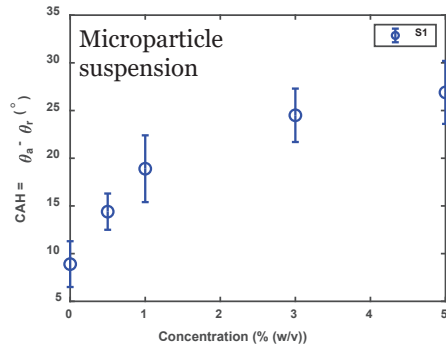


S. Shyam S. Misra
MAGIC AT INTERFACES

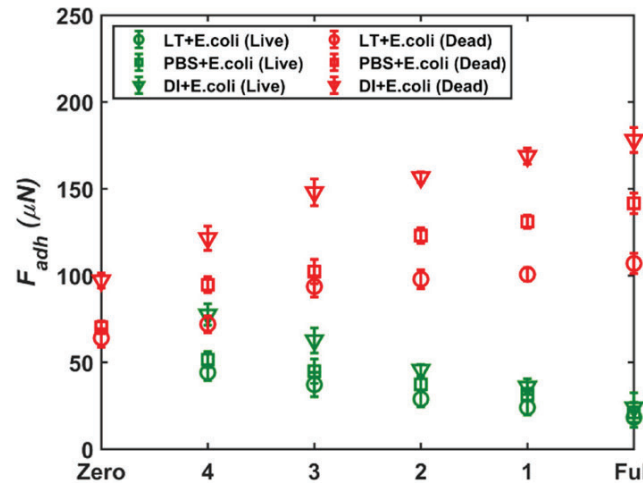
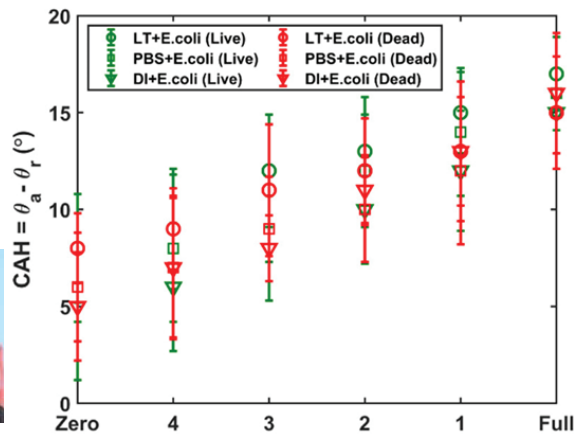
S. Shyam*, S. Misra*, S.K. Mitra, *Journal of Colloid And Interface Science* **2022**, 630, 322-333

Bacterial Adhesion: a tricky affair

Increasing CAH with concentration increment for both live & dead



However,



	Conc.	CAH	F_{adh}
Microparticle suspension	↑	↑	↑
Dead bacteria	↑	↑	↑
Live bacteria	↑	↑	↓



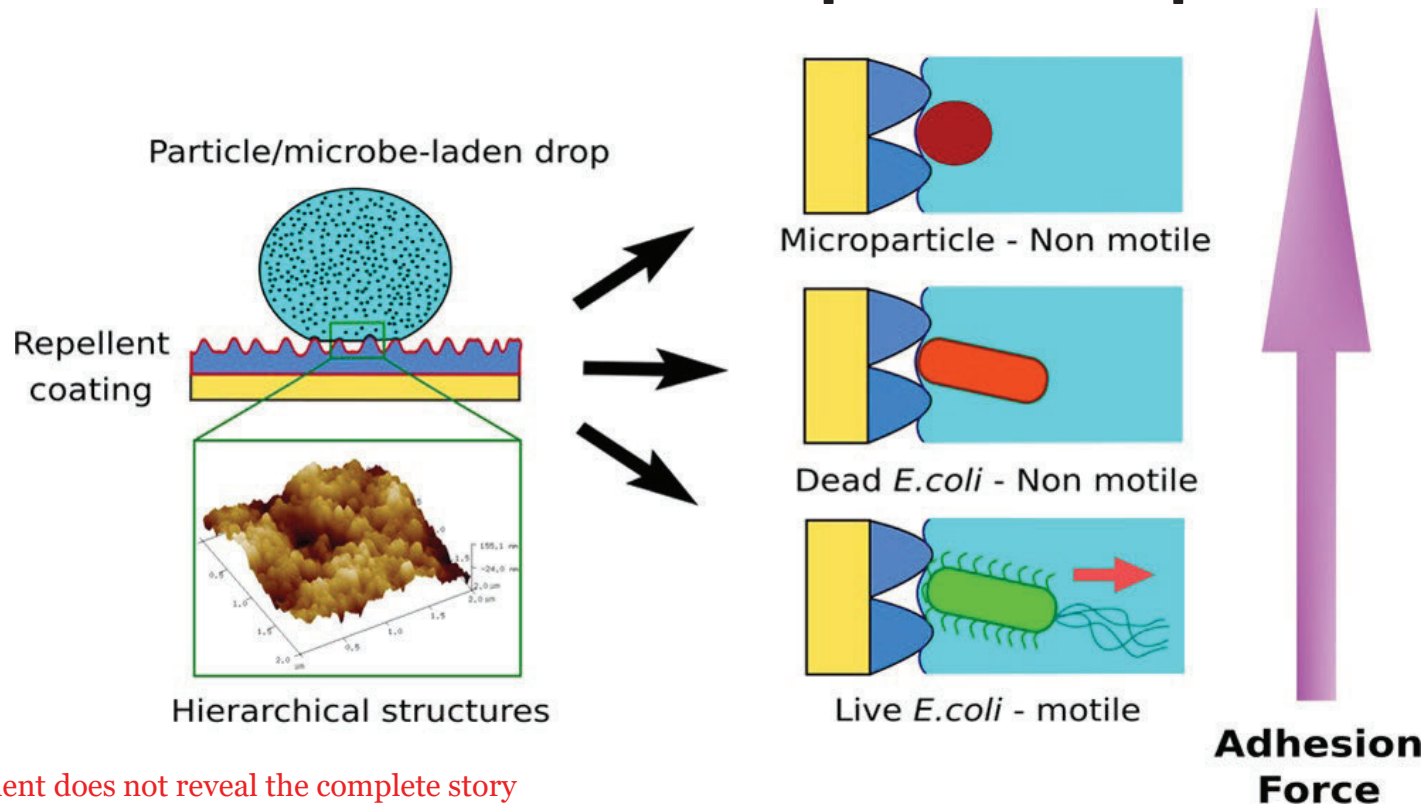
K. R. Melayil

K. R. Melayil, S. Misra, & S.K. Mitra, *Langmuir* 2021, 37(4), 1588–1595.
 K. R. Melayil, S. Misra, & S.K. Mitra, *Langmuir* 2020, 36(45), 13689–13697

MAGIC AT INTERFACES



Makes us wonder: Are bacteria and microparticles comparable?

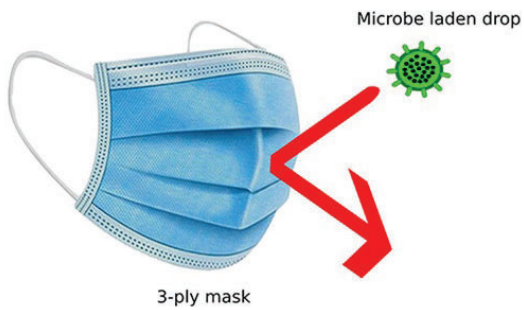


- CA measurement does not reveal the complete story
- Microparticles can not be used as a proxy for living bacteria – the mechanism of interaction is much intricate

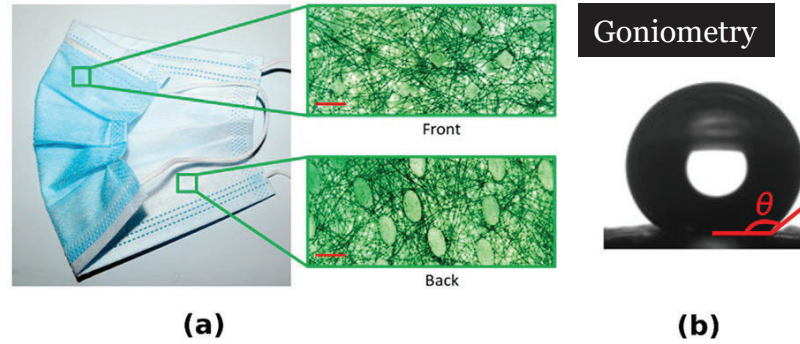
K. R. Melayil, S. Misra, & S.K. Mitra, *Langmuir* **2021**, 37(4), 1588–1595.
 K. R. Melayil, S. Misra, & S.K. Mitra, *Langmuir* **2020**, 36(45), 13689–13697

And then we get a virus laden drop : Wetting, adhesion and COVID-19

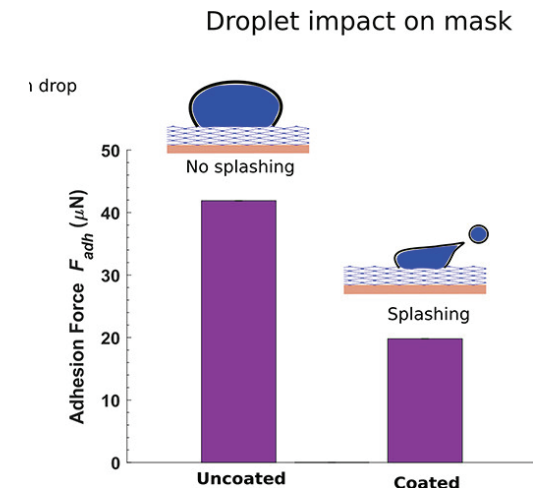
The problem



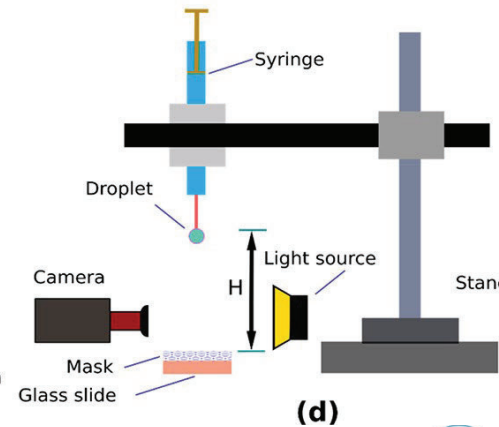
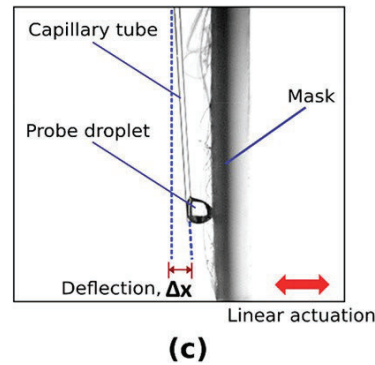
Possible solution avenues



Understanding adhesion is key



Adhesion measurements



Impact experiments

Now virus....

Nanoparticles might not be a suitable proxy for viruses

Establishment of a host cell line

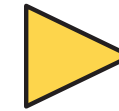
Cell seeding and transfection of the viral load onto healthy cells

Onset of cell cytopathy and subsequent collection of viral stock

Interface science experimentation

Healthy lung epithelial cells

Cells with prominent viral cytopathy

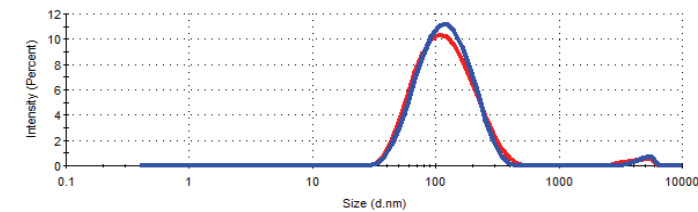


Repellent surface

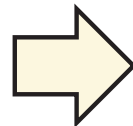
Undiluted viral load –
~10000 TCID50/ml

	Size (d.nm):	% Intensity:	St Dev (d.nm):
Z-Average (d.nm): 100.2	Peak 1: 129.8	98.1	61.88
PdI: 0.280	Peak 2: 4841	1.9	704.0
Intercept: 0.938	Peak 3: 0.000	0.0	0.000
Result quality: Good			

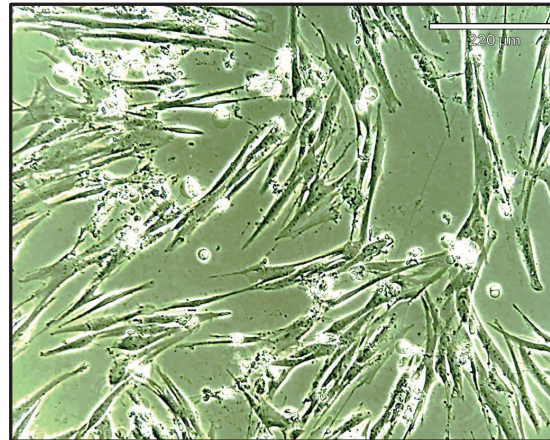
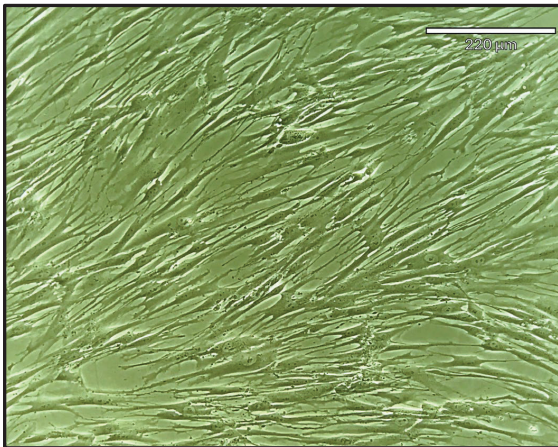
Size Distribution by Intensity



Viral transfection



**Ongoing work*



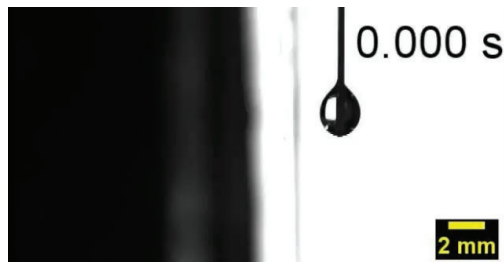
S. Misra

MAGIC AT INTERFACES



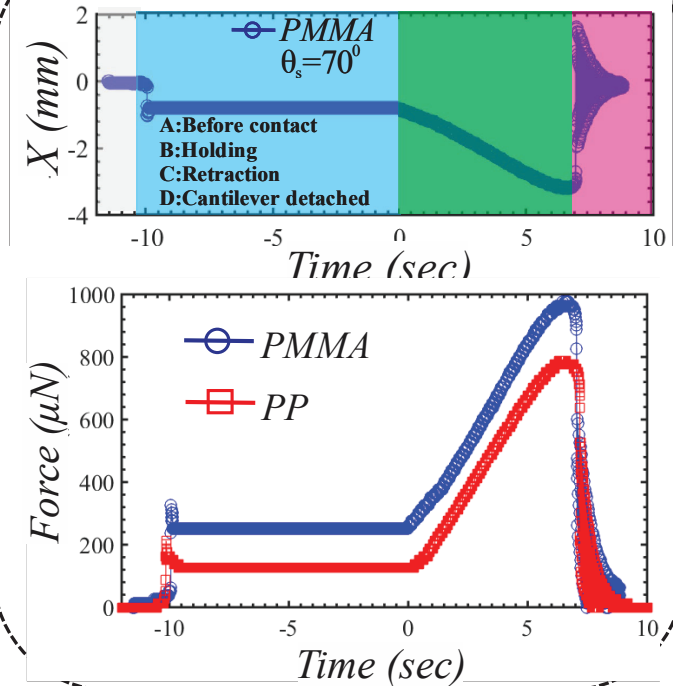
Revisiting limitations of existing adhesion measurement techniques

How to use the technique for characterizing high-energy surfaces, where a complete pull-off of the probe droplet could not be observed?



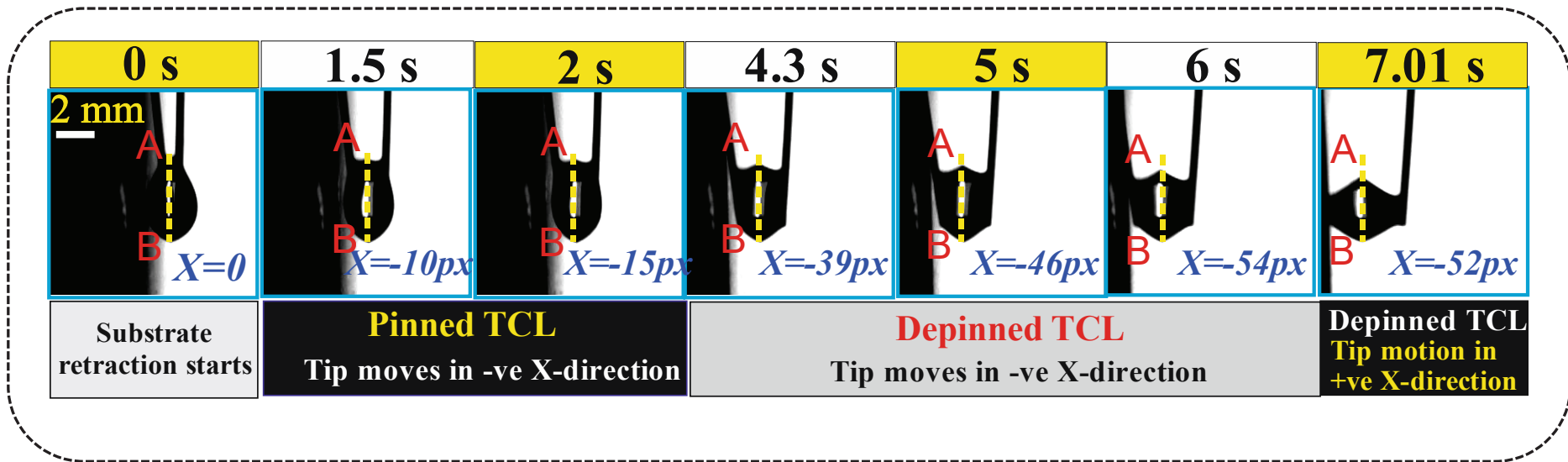
Adhesion measurement on a high-energy surfaces such as a PMMA substrate

For such case, what point in the force-time curve should we infer as the maximum adhesion force?



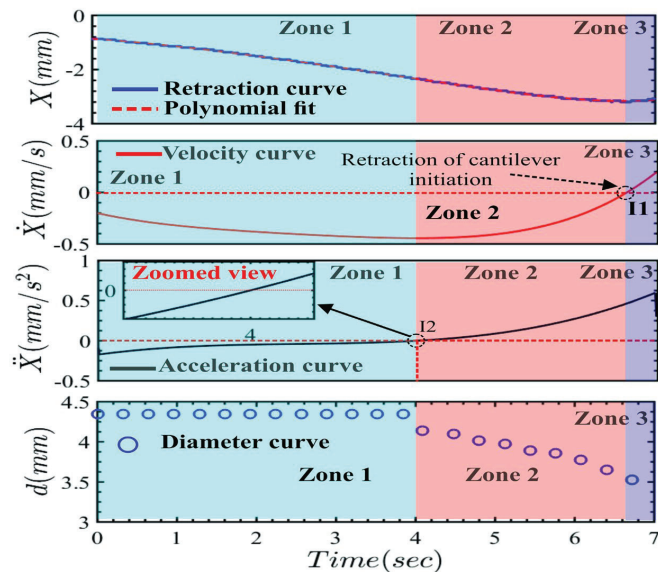
A modified technique

- Even for high-energy substrate a clear depinning could be observed
- Can we use the force corresponding to the point of depinning as the maximum adhesion force.

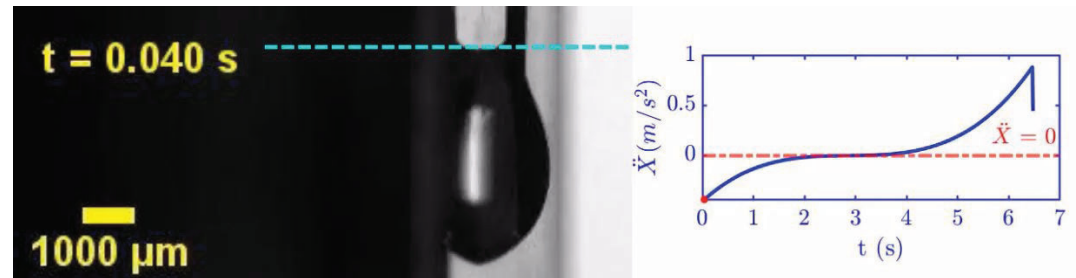


A modified technique

Even if depinning is the criteria, how do you correlate the motion of the cantilever with the onset of depinning?



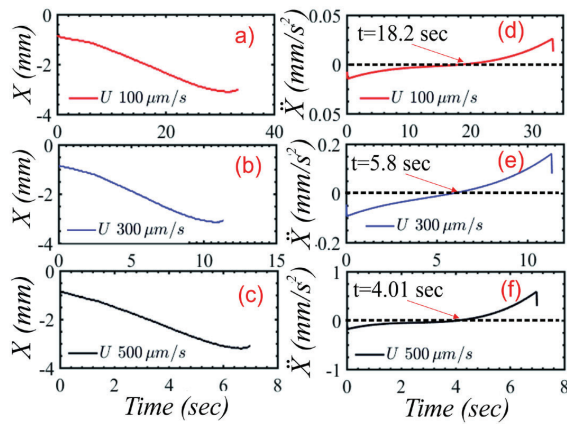
Temporal variation of the displacement (X), velocity (\dot{X}), acceleration (\ddot{X}) of the cantilever tip and the contact diameter of the probe droplet during the retraction of the test substrate



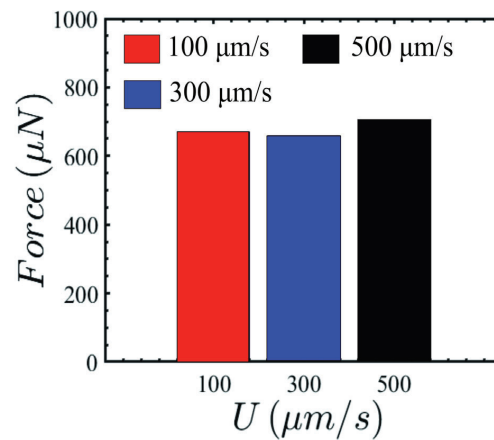
Onset of depinning corresponds to $\ddot{X} = 0$

Universality of the technique

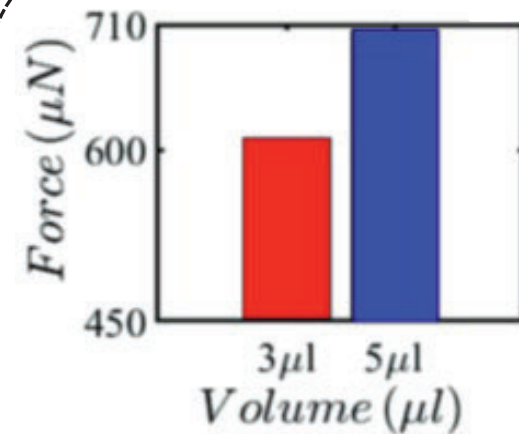
Force corresponding to the onset of depinning is the characteristic adhesion force.



The retraction and the corresponding acceleration curves for various substrate velocities



Adhesion force corresponding to the various substrate velocities



Adhesion force corresponding to various volumes of probe droplet

Wetting of 2D materials

The debate

nature
materials

LETTERS

PUBLISHED ONLINE: 22 JANUARY 2012 | DOI: 10.1038/NMAT3228

Wetting transparency of graphene

Javad Rafiee¹, Xi Mi², Hemtej Gullapalli³, Abhay V. Thomas¹, Fazel Yavari¹, Yunfeng Shi², Pulickel M. Ajayan^{3*} and Nikhil A. Koratkar^{1,2*}

We report that graphene coatings do not significantly disrupt the intrinsic wetting behaviour of surfaces for which surface-water interactions are dominated by van der Waals forces. Our contact angle measurements indicate that a graphene monolayer is wetting-transparent to copper, gold or silicon, but not glass, for which the wettability is dominated by short-range chemical bonding. With increasing number of graphene layers, the contact angle of water on copper gradually transitions towards the bulk graphite value, which is reached for ~6 graphene layers. Molecular dynamics simulations and theoretical predictions confirm our measurements and indicate that graphene's wetting transparency is related to its extreme thinness. We also show a 30–40% increase in condensation heat transfer on copper, as a result of the ability of the graphene coating to suppress copper oxidation without disrupting the intrinsic wettability of the surface. Such an ability to independently tune the properties of surfaces without disrupting their wetting response could have important implications in the design of conducting, conformal and impermeable surface coatings.

Graphene is a single-atom-thick sheet of sp²-hybridized carbon atoms arranged in a hexagonal honeycomb lattice. It possesses a unique combination^{1,2} of high specific surface area, chemical

film was transferred onto both Si and Au substrates. Films with a varying number of graphene layers (*N*), from monolayer to *N* > 10, were also deposited on Cu and glass substrates. Control of the number of layers was carried out by varying the growth time of CVD³ (as demonstrated in our previous work^{4,5}). Atomic force microscopy (AFM) and scanning electron microscopy (SEM) gave estimates of the number of graphene layers in each sample. Graphene-coated Cu and glass samples with *N* values ranging from 1, 1–2, 2–3, 4–6, 6–9, 8–12 and 10–15 were prepared. Figure 1a–c shows optical micrographs of large-area graphene film deposition on Cu, glass and Si, respectively. The deposited graphene is several cm in in-plane dimensions and forms a uniform conformal coating with no physical breaks. A Raman spectroscopy study (using 514 nm wavelength excitation) was used to confirm the approximate number of graphene layers on the Cu substrates. Figure 1d shows measured Raman spectra for the 2D peak for graphene films with a varying number of layers. A clear shift in the position of the 2D peak with number of layers is observed (Fig. 1d,e), from ~2,680 cm⁻¹ for monolayer graphene to ~2,715 cm⁻¹ for the *N* > 10 sample. These results are consistent with the literature; for example, Ferrari *et al.*⁶ have reported that, as the number of layers in graphene films is reduced, the 2D peak shifts towards a lower frequency range, and for single-layer graphene it ranges between 2,650 and 2,700 cm⁻¹.

Wetting transparent?

PRL 109, 176101 (2012)

PHYSICAL REVIEW LETTERS

week ending
26 OCTOBER 2012

Breakdown in the Wetting Transparency of Graphene

Chih-Jen Shih,¹ Qing Hua Wang,¹ Shangchao Lin,^{1,2,*} Kyoo-Chul Park,² Zhong Jin,¹ Michael S. Strano,¹ and Daniel Blankshtein^{1,†}

¹Department of Chemical Engineering, Massachusetts Institute of Technology, Cambridge, Massachusetts 02139, USA

²Department of Mechanical Engineering, Massachusetts Institute of Technology, Cambridge, Massachusetts 02139, USA

(Received 21 August 2012; published 24 October 2012)

We develop a theory to model the van der Waals interactions between liquid and graphene, including quantifying the wetting behavior of a graphene-coated surface. Molecular dynamics simulations and contact angle measurements were also carried out to test the theory. We show that graphene is only partially transparent to wetting and that the predicted highest attainable contact angle on a graphene-coated surface is 96°. Our findings reveal a more complex picture of wetting on graphene than what has been reported recently as complete “wetting transparency.”

DOI: 10.1103/PhysRevLett.109.176101

PACS numbers: 68.08.Bc, 68.03.Cd, 68.65.Pq

Partially transparent?

Wettability of Graphene

Rishi Raj,[†] Shalabh C. Maroo,[‡] and Evelyn N. Wang^{*,†}

[†]Device Research Laboratory, Department of Mechanical Engineering, Massachusetts Institute of Technology, Cambridge, Massachusetts 02139, United States

[‡]Department of Mechanical and Aerospace Engineering, Syracuse University, Syracuse, New York 13244, United States

Our results which indicate that the underlying substrate has a negligible effect on the wettability of graphene-coated copper, silica, and glass substrates is now explained in the context of similar results in literature. For copper where van der Waals forces dominate, the experimental contact angle values for graphene coated copper in our work agrees with those reported in Rafiee *et al.*⁵⁶ However, the contact angle used for bare copper substrates differs in the models, which lead to discrepancies in the interpretation of the substrate effect. While we demonstrated through the comparison of our simulation results (using fundamental LJ parameters from literature⁵⁷) and previously reported controlled experiments⁵² that pristine copper underneath the CVD grown graphene is superhydrophilic with apparent contact angles of 0°, Rafiee *et al.*⁵⁶ used the large experimental contact angle values (84–85°) on copper with native oxide layer and contaminants in ambient as the bare substrate wettability in their model. Accordingly, if the fundamental LJ parameters⁵⁷ resulting in pristine copper substrate wettability⁵² was used, the effect of the underlying substrate on the wettability even for a monolayer graphene coating on copper would be negligible.

In literature for monolayer graphene on glass and SiO₂ (where both van der Waals and electrostatic forces due to partial charges dominate), static contact angle measurements

cleaned silica surface in Shih *et al.*⁵⁰ however, demonstrate the potential of unobtrusive graphene coatings for surface wettability. Physical understanding of wettability on such plasma cleaned surfaces with free charges remains absent in literature and requires additional theoretical and modeling efforts to elucidate the underlying physics.

Conclusions. We demonstrated that copper, glass, and silica substrates coated with an atomically thin 2D material graphene matches the wettability of 3D bulk graphite. The advancing contact angle was found to be independent of the number of layers of graphene sheets and was in good agreement with our molecular dynamics simulation and theoretical calculations. The receding contact angle, however, was governed by the defects in as-grown and transferred graphene sheets, leading to significant contact angle hysteresis. As a result, static contact angle measurements for wettability and surface energy characterization on such surfaces cannot solely be used. Continuum models for interfacial and adsorption energy calculations were shown to be inaccurate due to the underestimation of the solid–liquid equilibrium distances in graphene-coated substrates. The fundamental understanding of graphene–water interactions elucidated in this study is an important step towards developing graphene assisted surface-coatings for heat transfer and microfluidics devices.

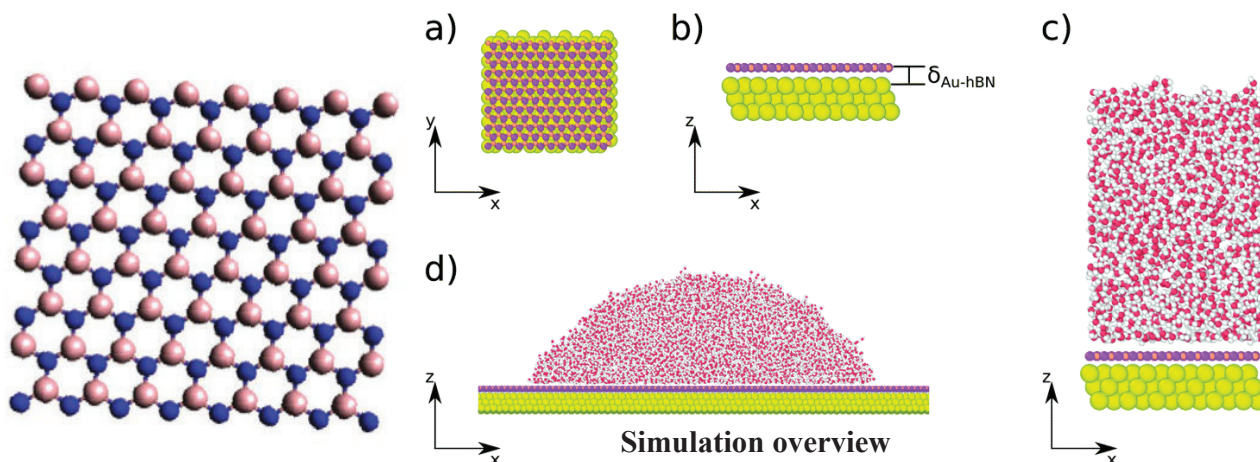
Or opaque?

PAGE 44

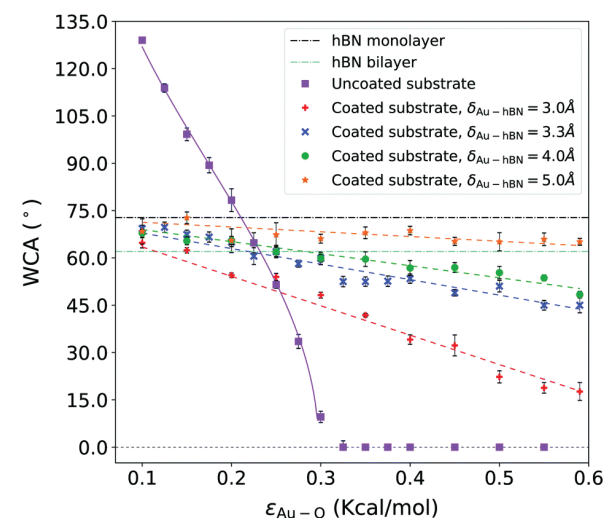


UNIVERSITY OF
WATERLOO

hBN: looking ahead of graphene



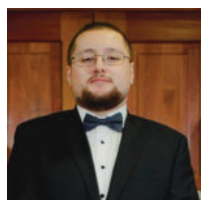
Wetting translucency effect is observed
On unstructured surfaces



What about the wetting of nanostructured hBN surfaces?

Despite similar interfacial structure, hBN presents higher friction to water compared to carbon-based nanostructures (CNT and Graphene)

Tocci, et al. *Nano letters* 14.12 (2014): 6872-6877.
Joseph and Aluru. *Nano letters* 8.2 (2008): 452-458.



E. Wagemann

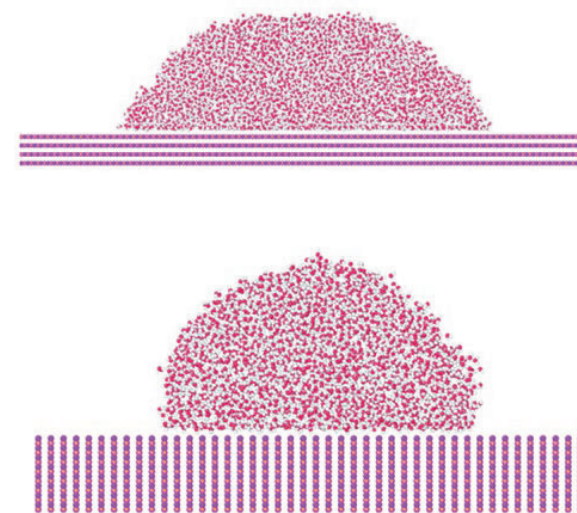
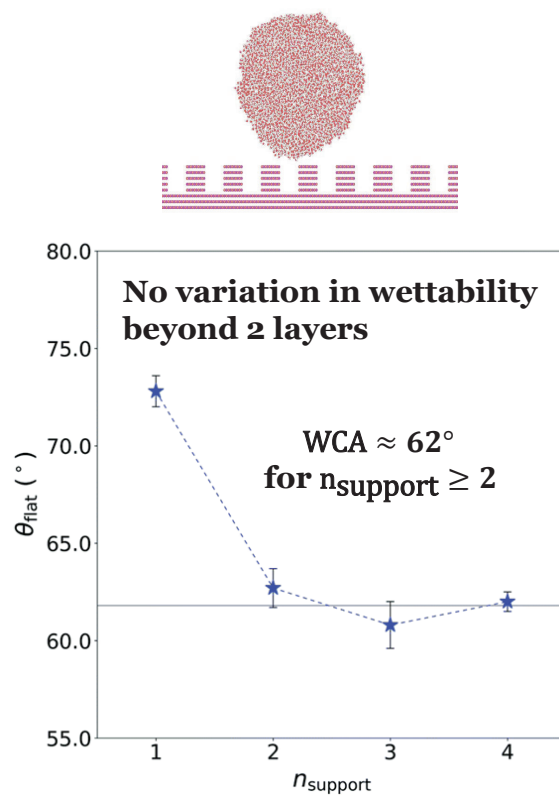
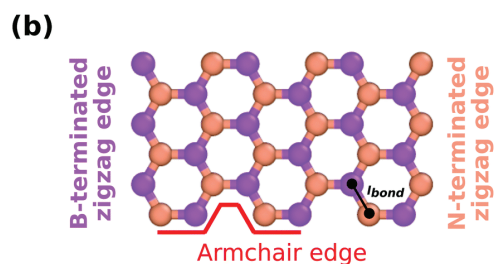
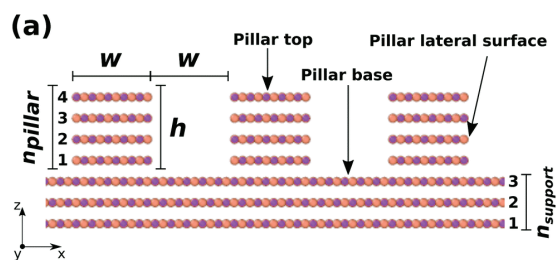
Wagemann et al., *Phys. Chem. Chem. Phys.* 2020;22(15):7710-7718



Electrostatic interactions between water and hBN atoms play a key role



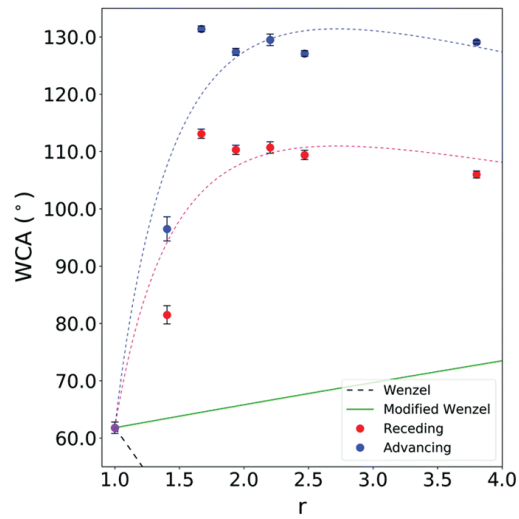
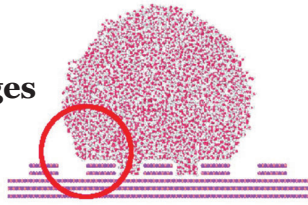
Nanostructured hBN - tunable wettability regime



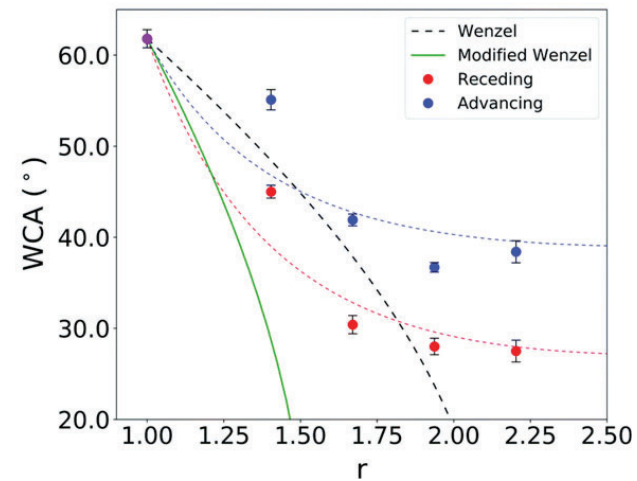
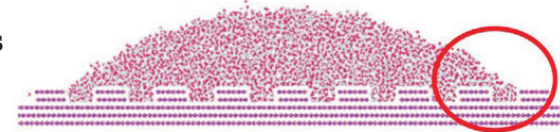
Hydrophobic lateral (armchair) walls

Effect of nanostructured edges - armchair vs zigzag

Armchair edges

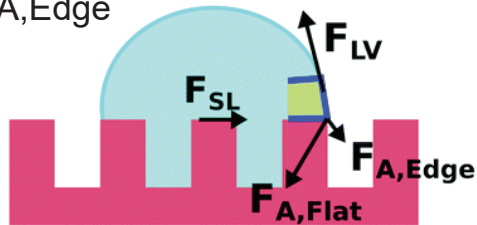


Zigzag edges



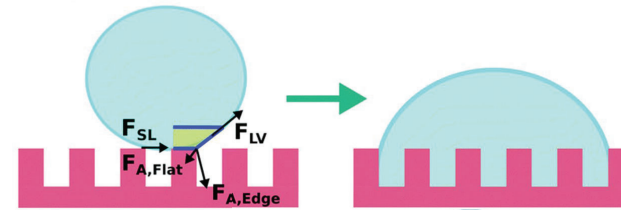
VS.

$$F_{A,Flat} > F_{A,Edge}$$



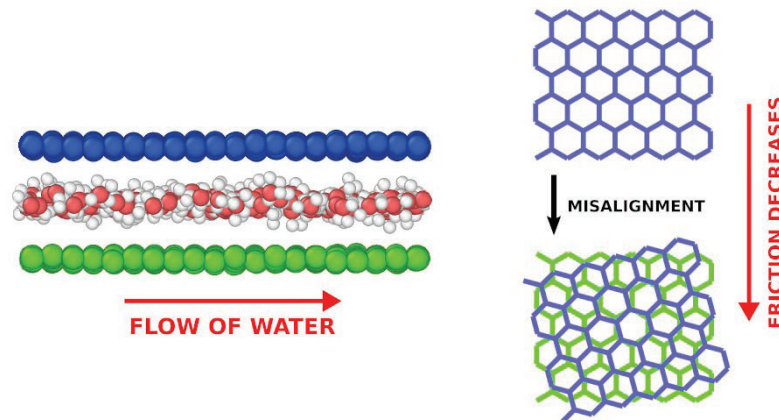
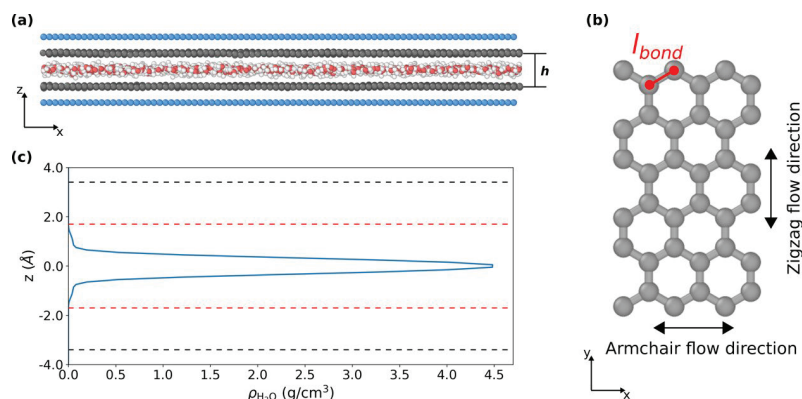
$$F_{A,Flat} < F_{A,Edge}$$

Wenzel transition

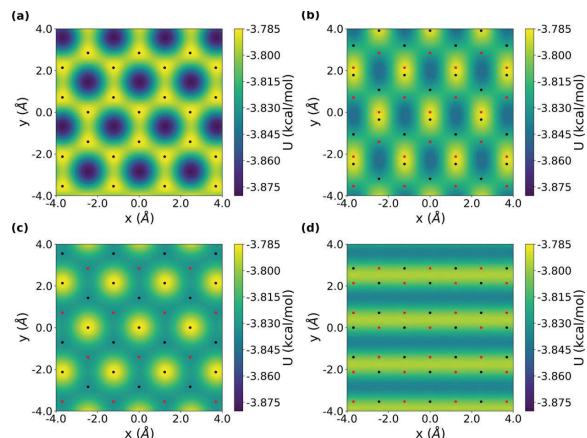


Water friction inside Ångström confinements

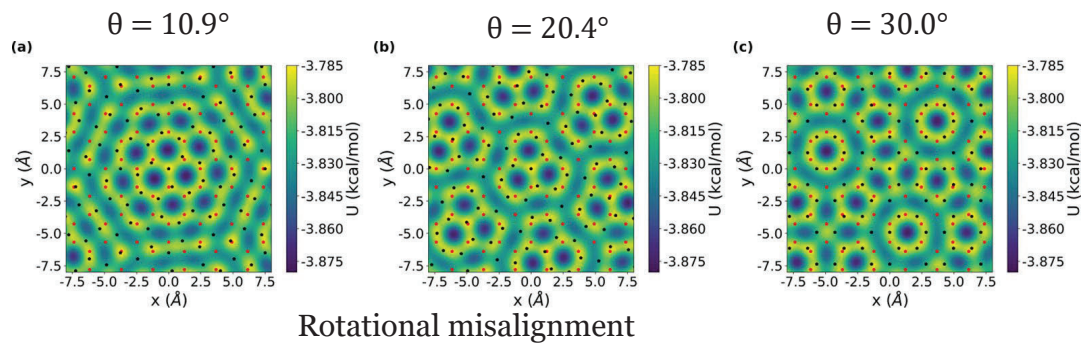
Types of misalignment: translational vs rotational



Potential energy landscape



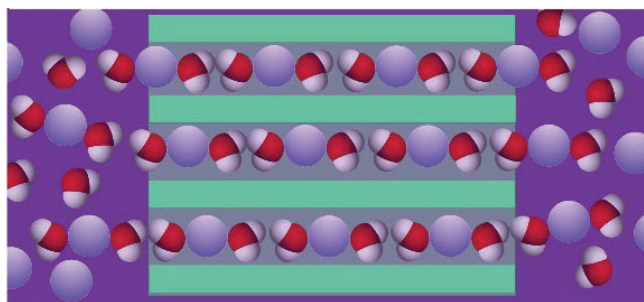
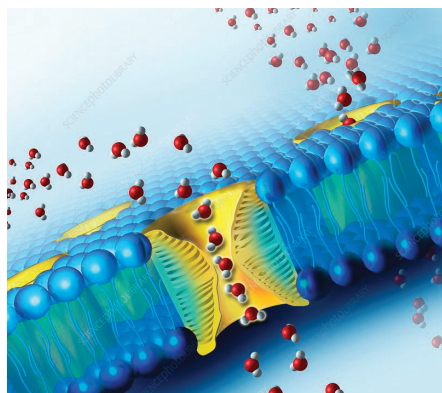
Translational misalignment



Rotational misalignment

Design efficient transport mechanism through Ångström channels via misalignment

Commercialization pathway



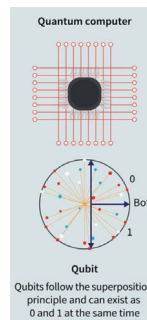
 Water Molecule  Trapped Ion (Cs⁺ or Na⁺)

Aquabits – Revolutionizing Trapped ion technology

Patents:

US 2021/0308624 A1 Published: October 7, 2021

PCT WO 2021/195788 A1 Published: October 7, 2021



Aquabits
www.AquabitsQ.com
skmitra@uwaterloo.ca



Thank you

Micro & Nano-scale Transport Laboratory
Rm 1512, Mike & Ophelia Lazaridis Quantum-Nano Centre
200 University Avenue West
Waterloo, ON, Canada N2L 3G1

